Neutron Star Astrophysics at the Crossroads: Magnetars and the Multimessenger Revolution
Proceedings IAU Symposium No. 363, 2023
E. Troja & M. G. Baring, eds.
doi:10.1017/S1743921322000904

The simulations of early kilonova emission from neutron star mergers

Smaranika Banerjee[1], Masaomi Tanaka[1], Kyohei Kawaguchi[2], Daiji Kato[3] and Gediminas Gaigalas[4]

[1]Astronomical Institute, Tohoku University,
Aoba, Sendai 980-8578, Japan
email: smaranikab@astr.tohoku.ac.jp

[2]Institute for Cosmic Ray Research, The University of Tokyo,
5-1-5 Kashiwanoha, Kashiwa, Chiba 277-8582, Japan

[3]National Institute for Fusion Science, National Institutes of Natural Sciences, Department of Advanced Energy Engineering Science, Kyushu University,
Oroshi-cho, Toki, Gifu 509-5292, Japan

[4]Institute of Theoretical Physics and Astronomy, Vilnius University, Saulėtekio av. 3,
LT-10257 Vilnius, Lithuania

Abstract. In the neutron-star mergers, the radioactive decay of freshly synthesized heavy elements produces emissions in the ultraviolet-optical-infrared range, producing a transient called kilonova. The observational properties of the kilonova depend on the bound-bound opacity of the heavy elements, which was largely unavailable for the conditionssuitable at an early time ($t < 1$ day). In this article, I share some of our recent progress on modeling the early kilonova light curve, focusing on the atomic opacity calculation.

Keywords. opacity, stars: neutron, radiative transfer

1. Introduction

In the neutron star mergers, heavy elements are synthesized via rapid neutron capture (r-process, Lattimer & Schramm 1974). The radioactive decay of such elements produces emissions in the ultraviolet-optical-infrared (UVOIR) range, called a kilonova (Li & Paczynski 1998). Such a kilonova (AT2017gfo, Coulter, D. A. *et al.* 2017) is observed for the first time as a follow-up observation of the gravitational wave event GW170817 (Abbott *et al.* 2017). The observed signal for AT2017gfo at time $t > 1$ day is well explained to be powered by the radioactive decay of heavy elements (Tanaka et al. 2017, Kasen et al. 2017). However, the emission mechanism at the early time ($t < 1$ day) did not reach strong consensus (Arcavi 2018).

The shape of the kilonova light curve depends on the opacity. In kilonova, the most dominant opacity component comes from the bound-bound transitions. Calculation of the bound-bound opacity requires atomic data, which was unavailable corresponding to the hot, highly ionized ejecta at early time (typical ionization up to 10^{th} (or XI in spectroscopic notation, will be used throughout the article), corresponding to temperature $T \sim 10^5$ K at $t \sim 0.1$ day). Hence, the realistic simulation of the early kilonova was not possible.

We perform the first systematic atomic and opacity calculation for the highly ionized (up to XI) heavy elements (Ca to Lu, $Z = 20 - 71$). Thanks to the new atomic opacity,

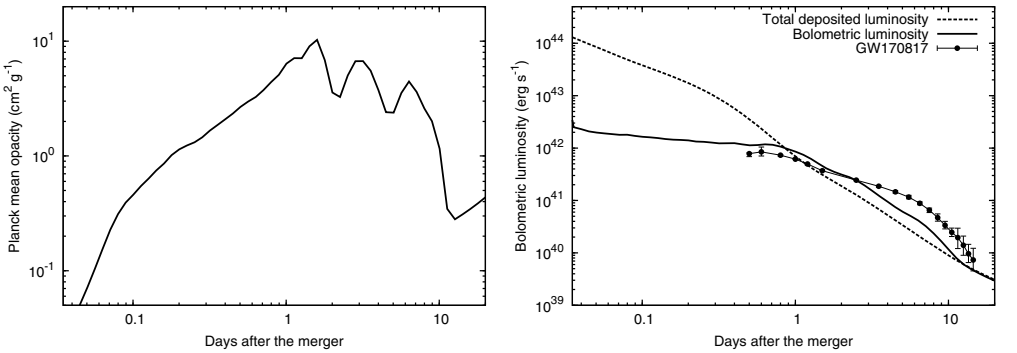

Figure 1. Left panel: The Planck mean opacity (bound-bound) evolution for a binary neutron star merger with a total ejecta mass of $0.05M_{\odot}$ and light $r-$process abundance (suitable for the polar kilonova) at an ejecta velocity of $v = 0.1c$. **Right panel:** Deposited and bolometric luminosity (dashed and solid curves) for the same model. The bolometric light curve for GW170817/AT2017gfo is shown for comparison (Waxman et al. 2018).

calculation of the first realistic light curve of early kilonova (starting from $t \sim 0.1$ day) is possible.

2. Elemental abundance in the neutron star merger

The neutron star merger has several mass ejection channels (Shibata & Hotokezaka 2019), producing multiple ejecta components. Elemental abundance varies among different ejecta components. The heaviest elements including lanthanides ($Z = 57 - 71$) are distributed near to the equatorial plane (Bauswein et al. 2013a), whereas light $r-$process elements are distributed more isotropically or near to the pole (Metzger & Fernandez 2014, Miller et al. 2019). Differences in the elemental abundances cause difference in the opacity, introducing a viewing angle dependence in kilonova.

3. Polar kilonova

We model the early kilonova light curve observed from the polar direction for a simple 1D spherical ejecta model with a power-law density structure (Metzger et al. 2010. The total mass of the ejecta is taken to be $0.05M_{\odot}$, with the maximum velocity up to 0.2c. The abundance pattern is considered to be light r-process elements ($Z = 20 - 56$). Our model parameters are typical for that of the disk wind ejecta (Metzger & Fernandez 2014).

We calculate the opacity for our disk wind model using the expansion opacity formalism (Sobolev V. V. 1960). We calculate the necessary atomic data for all the light r-process elements ($Z = 20 - 56$) for a maximum ionization up to XI using Hebrew University Lawrence Livermore atomic code (HULLAC, Bar-Shalom, A. et al. 2001). More details of the atomic opacity calculation can be found in Banerjee *et al.* 2020. Using the new opacity, we calculate the early kilonova light curve using a Monte Carlo radiative transfer code (Tanaka & Hotokezaka 2013).

The Planck mean opacity changes from $\kappa \sim 0.5\,\mathrm{cm^2\,g^{-1}}$ at $t = 0.1$ day to $\kappa \sim 5\,\mathrm{cm^2\,g^{-1}}$ at $t = 1$ day (Figure 1). This is because as the ejecta expands, the ejecta condition such as density, temperature (and hence the ionization) changes. Our work shows that the assumption of the constant opacity used by several previous works to model early kilonova (for example, Piro & Kollmeier 2018) is not true.

The bolometric luminosity deviates from the total deposited luminosity (solid and dashed lines, respectively, in Figure 1) at the early time ($t < 1$ day). This is due to

https://doi.org/10.1017/S1743921322000904 Published online by Cambridge University Press

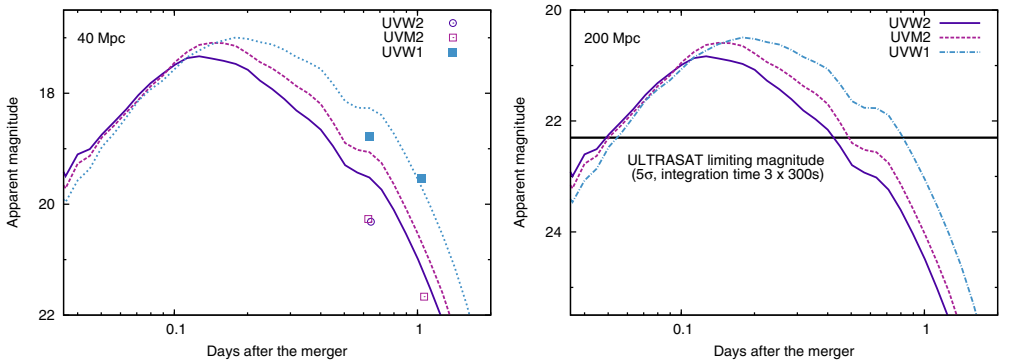

Figure 2. Left panel: The apparent UV light curve for a polar kilonova at a same distance as GW170817/AT2017gfo (data from Evans, P. A. *et al.* 2017 is shown for comparison). **Right panel:** Apparent UV light curve for a GW170817/AT2017gfo-like source at 200 Mpc is shown.

the fact that in the early time, the ejecta is still optically thick, and the photons can escape only from the outermost layer. With time, the ejecta expands and more photons can escape. Finally, the bolometric luminosity follows the deposited luminosity in $t \sim 10$ days.

Comparison with GW170817/AT2017gfo

Our model light curve shows good agreement with the early bolometric luminosity of GW170817/AT2017gfo (Figure 1, data is from Waxman et al. 2018), which is observed near to the pole (Abbott *et al.* 2017, Finstad et al. 2018). Moreover, our model is sufficient to reproduce the early UV observation of GW170817/AT2017gfo (Figure 2, data is taken from Evans, P. A. *et al.* 2017). Hence, our simple radioactive decay model with an ejecta mass of $0.05 M_{\odot}$ and light $r-$process abundance can reproduce the early bolometric and UV light curve of the kilonova GW170817/AT2017gfo.

Future prospects

Finally, we discuss the future detection prospects of polar kilonova. Our model shows that for a GW170817/AT2017gfo-like source at 200 Mpc, UV emission peaks at $t \sim 4$ hours with an apparent magnitude of ~ 20.5 (Figure 2). Such signal is detectable by existing facility like Swift (Roming et al. 2005), provided the source can be detected early enough. Also, now with the wide field UV survey like Ultraviolet Transient Astronomy Satellite (ULTRASAT, Sagiv *et al.* 2014) coming up (limiting magnitude ~ 22 mag (5σ) for an exposure time of 900 s, Figure 2), many more such detection will be possible in the near future.

4. Equatorial kilonova

To model the equatorial kilonova at an early time ($t \sim 0.1$ day), we require the atomic opacity calculation for all the highly ionized (up to XI) heavy elements, including lanthanides ($Z = 57 - 71$). Lanthanides are the elements with the open $f-$shell, presence of them has significant impact on the opacity (see Tanaka et al. 2020 for opacity of the low-ionized lanthanides). In this article, we discuss the atomic opacity trend for the highly-ionized lanthanides, taking Eu ($Z = 63$) as an representative element.

The atomic data and the bound-bound opacity for lanthanides are calculated in a similar way as mentioned in Section 3, with the difference that here we use a single element ejecta model with the fixed density $\rho = 10^{-10}$ g cm^{-3} (typical density at $t \sim 0.1$ day). Although the single elemental abundance does not represent a realistic condition, it helps to qualitatively understand the effect of the presence of lanthanides in the ejecta.

https://doi.org/10.1017/S1743921322000904 Published online by Cambridge University Press

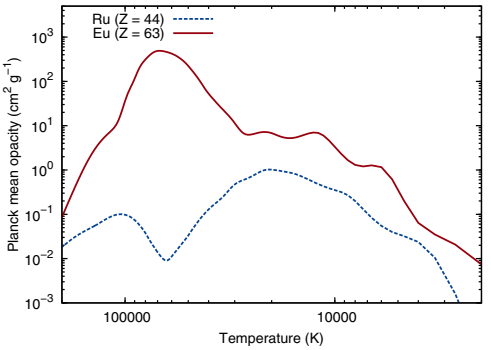

Figure 3. The Planck mean opacity (bound-bound) as a function of temperature for the light $r-$process element Ru ($Z = 44$, dashed) and the lanthanide element Eu ($Z = 63$, solid).

Figure 3 shows our result for the Planck mean opacity for the lanthanide element Eu as a function of the temperature. The temperature is plotted in the reverse axis to follow the time evolution (the temperature decreases with time). The opacity at the high temperature corresponds to the opacity at the early time. The peak opacity value for Eu reaches up to $\sim 10^3$ cm^2 g^{-1} at $T \sim 70000$ K, which is exceptionally high (the opacity peak for the light $r-$process elements Ru ($Z = 44$) reaches only up to 0.1 cm^2 g^{-1} under the same condition).

Our study shows that the presence of the lanthanides in the ejecta increases the opacity significantly at the early time. Such a high opacity is likely to cause strong suppression in the early UV emission, which will be explored in the future work.

References

Abbott, B. P., Abbott, R., Abbott, T. D., et al. 2017, *PhRvL*, 119, 161101
Arcavi, I. 2018, *ApJ letter*, 855, L23
Banerjee, S., Tanaka, M., Kawaguchi, K., Kato, D., Gaigalas, G. 2020, *ApJ*, 901, 29
Bar-Shalom, A., Klapisch, M., Oreg, J. 2001, *JQSRT*, 71, 169
Bauswein A., Baumgarte T. W., Janka H.T. 2013, *Phys. Rev. Lett.*, 111, 131101
Brown, P. J., Breeveld, A. A., Holland, S., Kuin, P., et al. 2014, *Ap&SS*, 354, 89
Coulter, D. A., Foley, R. J., Kilpatrick, C. D., et al. 2017, *Science*, 358, 1556
Evans, P. A., Cenko, S. B., Kennea, J. A., et al. 2017, *Science*, 358, 1565
Finstad, D., De, S., Brown, D.A., et al. 2018, *ApJL*, 860, L2
Kasen, D., Metzger, B., Barnes, J., Quataert, E., Ramirez-Ruiz. 2017, *Nature*, 551, 80
Kawaguchi, K., Shibata, M., Tanaka, M. 2020, *ApJ*, 889, 171
Lattimer, J. M., & Schramm, D. N. 1974, *ApJL*, 192, L145
Li, L. X. & Paczynski, B. 1998, *ApJL*, 507, L59
Metzger, B. D., Martınez-Pinedo, G., Darbha, S., et al. 2010, *MNRAS*, 406, 2650
Metzger, B. D., & Fernandez, R. 2014, *MNRAS*, 441, 3444
Miller, J. M., Ryan, B. R., Dolence, J. C., et al. 2019, *Phys. Rev. D*, 100, 023008
Piro, A. L., Kollmeier, J. A. 2018, *ApJ*, 855, 103
Roming, P. W. A., Kennedy, T. E., Mason, K. O., et al. 2005, *SSRv*, 120, 95
Sagiv, I., Gal-Yam, A., Ofek, E. O., et al. 2014, *AJ*, 147, 79
Shibata, M., Hotokezaka, K. 2019, *Annu. Rev. Nucl. Part. Sci.*, 69, 41
Sobolev, V. V. 1960, *Moving envelopes of stars*
Tanaka, M., Kato, D., Gaigalas, G., Kawaguchi, K., 2020, *MNRAS*, 496, 1369
Tanaka, M. & Hotokezaka, K. 2013, *ApJ*, 775, 113
Tanaka, M., Utsumi, Y., Mazzali, P. A., et al. 2017, *PASJ*, 69, 102
Waxman, E., Ofek, E. O., Kushnir, D., Gal-Yam, A. 2018, *MNRAS*, 481, 3423

https://doi.org/10.1017/S1743921322000904 Published online by Cambridge University Press